Journal of South American Earth Sciences 96 (2019) 102327

Contents lists available at ScienceDirect

Journal of South American Earth Sciences

journal homepage: www.elsevier.com/locate/jsames

# Fossildiagenesis and ontogenetic insights of crocodyliform bones from the Adamantina Formation, Bauru Basin, Brazil

Isadora Marchetti[a,**], Fresia Ricardi-Branco[a,***], Flavia Callefo[b], Rafael Delcourt[a,c,*], Douglas Galante[b], Isabela Jurigan[a], Ismar S. Carvalho[d], Sandra A.S. Tavares[e]

[a] Universidade Estadual de Campinas (UNICAMP), Instituto de Geociências, CidadeUniversitária, Rua Carlos Gomes, 250, 13083-855, Campinas, SP, Brazil
[b] Laboratório Nacional de Luz Síncrotron, Centro Nacional de Pesquisas em Energia e Materiais, Rua Giuseppe Máximo Scolfaro, 10.000, Polo II de Alta Tecnologia de Campinas, 13083-100 Campinas, São Paulo, Brazil
[c] Museu Nacional, Universidade Federal do Rio de Janeiro, Departamento de Geologia e Paleontologia, 20940-040 Rio de Janeiro, RJ, Brazil
[d] Universidade Federal do Rio de Janeiro, Centro de Ciências Matemáticas e da Natureza, Instituto de Geociências, Departamento de Geologia, Cidade Universitária, Ilha do Fundão, Av. Athos da Silveira Ramos, 274, Bloco G, 21941-916 Rio de Janeiro, RJ, Brazil
[e] Museu de Paleontologia "Prof. Antonio Celso de Arruda Campos", Praça do Centenário - s/n Centro, Monte Alto, SP, Brazil

ARTICLE INFO

*Keywords:*
Paleohistology
REEs
Cretaceous
Crocodile
Montealtosuchus

ABSTRACT

The histological analysis of fossil bones allows a taphonomic approach, especially to fossildiagenesis. We studied the femur, vertebra, and osteoderm of the crocodyliform *Montealtosuchus arrudacamposi* (Adamantina Formation; Late Cretaceous), to make inferences of the sequence of the diagenetic processes. Cross-sections of the bones and the rock matrix that fills the medullar cavity were analyzed under a scanning electron microscopy with compositional analysis (SEM/EDS) and μ-X-Ray fluorescence (μ-XRF). The microstructural pattern of the femur and vertebra was similar, with a transition from vascularized fibrolamellar internal cortex, with reticular and longitudinal canals to zonal lamellar in the outer, and a medullary cavity portion filled with quartz and other mineral grains. The osteoderm, however, presented a less vascularized cortex. In all samples were found the External Fundamental System (EFS), secondary osteons in the internal cortex and spongy tissue, and the transition from a fibrolamellar to a lamellar tissues, indicating that the individual reached ontogenetic maturity (adult/senescent) before they died. The compositional results showed that the samples mainly comprised calcium and phosphorus, which were homogeneously distributed. However, we inferred that these elements occurred during the formation of recrystallized and authigenic minerals. Iron, vanadium, and cerium are the elements found that occurred in the composition of the fossil remains during early diagenesis, and this process was observed to extend to the late diagenesis. Cerium was homogeneously distributed and incorporated to authigenic apatite. Iron and vanadium were restricted to the cortex. The presence of authigenic apatite and Rare Earth Elements (REEs) in the samples supported that the diagenetic environment of the Adamantina Formation was alkaline. Furthermore, it suggested an association with a groundwater environment that have allowed and facilitated the well preservation of fossil vertebrates in this geological formation.

## 1. Introduction

The record of cretaceous crocodyliforms from Brazil is expressive, especially considering the Bauru Group where several Notosuchia were unearthed in the last years (e.g. Martinelli et al., 2018; Pol et al., 2014). The taxa Notosuchidae, Trematochampsidae, Baurusuchidae and Peirosauridae are the main known families recovered in Brazil (Martinelli et al., 2018; Pol et al., 2014; Martine, 2013; Nascimento and Zaher, 2010; Marinho, 2006; Carvalho et al., 2004). Several outcrops from the region of Monte Alto, São Paulo state (Fig. 1), revealed a high diversity

* Corresponding author. Universidade Estadual de Campinas (UNICAMP), Instituto de Geociências, CidadeUniversitária, Rua Carlos Gomes, 250, 13083-855, Campinas, SP, Brazil.
** Corresponding author.
*** Corresponding author.
*E-mail addresses:* zamarchetti@gmail.com (I. Marchetti), fresia@ige.unicamp.br (F. Ricardi-Branco), flacallefo@gmail.com (F. Callefo), rafael.delcourt@gmail.com (R. Delcourt), douglas.galante@lnls.br (D. Galante), ismar@geologia.ufrj.br (I.S. Carvalho), sandraastavares@gmail.com (S.A.S. Tavares).

https://doi.org/10.1016/j.jsames.2019.102327
Received 6 May 2019; Received in revised form 22 August 2019; Accepted 27 August 2019
Available online 30 August 2019
0895-9811/ 

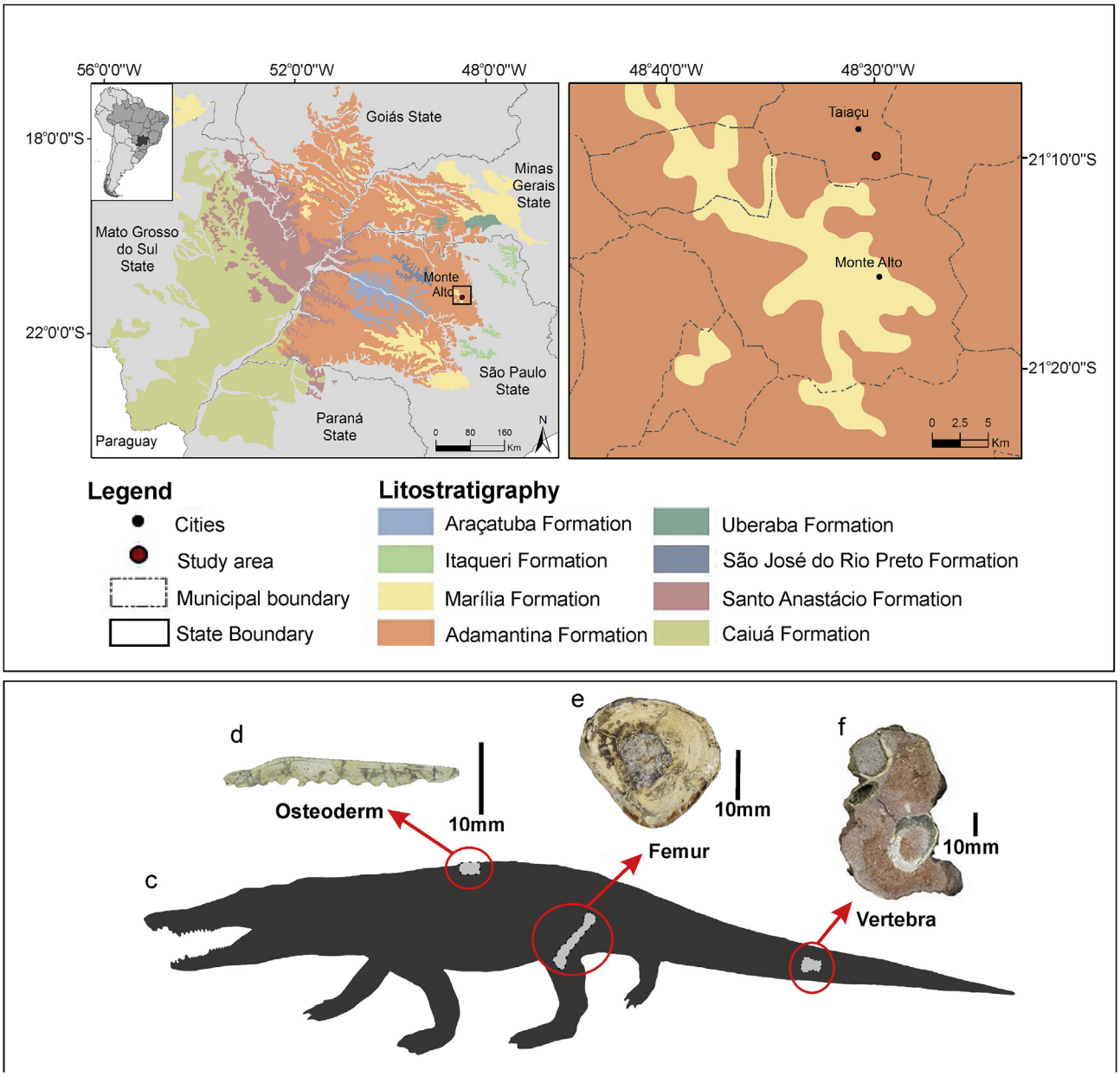


**Fig. 1.** Locality map of the Monte Alto municipality, in geological map of the Bauru Basin in Brazil (Modified from Menegazzo et al., 2016) and studied samples disposition in *Montealtosuchus*. C) Schematic drawing with the positioning of studied fossils within the silhouette; D) dorsal osteoderm (MPMA-0007/04); E) femur (DP2/176); F) caudal vertebra (DP2/177).

**Table 1**
Transversal diameters (in mm) of the *Montealtosuchus* samples.

| Samples | Medullar Cavity | Spongy Tissue | Compact Tissue |
|---|---|---|---|
| Femur (15 mm) | 2 | 2 | 4 |
| Vertebra (20 mm) | 10 | 2 | 3 |
| Osteoderm (4 mm) | – | 2 | 1 |

of crocodyliform fossils, which have been described in the last years, increasing the record of Brazilian notosuchians. These fossils belong to a wide variety of terrestrial species such as *Morrinhosuchus luziai* Iori and Carvalho (2009); *Caipirasuchus montealtensis* Andrade and Bertini (2008); *Caipirasuchus paulistanus* Iori and Carvalho (2011); *Barreirosuchus franciscoi* Iori and Garcia (2012), and *Montealtosuchus arrudacamposi* Carvalho et al. (2007), from the Upper Cretaceous. Among them, *Montealtosuchus*, a peirosaurid (Tavares et al., 2015), was found in association with several isolated fossil fragments that probably belonged to the same genus.

Recent studies focusing on preserved micro-structures of crocodyliform fossils have gathered information on physiology, ontogeny, mechanics and environment adaptations. (Andrade and Sayão, 2014; Sayão et al., 2016; Andrade and Bertini, 2008). These aspects can vary according to the different types of bones, their ontogenetic stages, and fossil diagenesis (Chinsamy-Turan, 2005). Without these aspects, most information about the growth rate and sexual maturity of these extinct species would remain unknown (Padian and Lamm, 2013). It is traditionally known that reptiles could have indeterminate growth (Chinsamy-Turan, 2005; Sparkman et al., 2007). Nevertheless, new evidences suggest the presence of the External Fundamental System (EFS) in Archosauria indicating a cessation of the growth when they reach late ontogenetic stages. (Klein et al., 2009; Woodward et al., 2011; Andrade and Sayão, 2014; Andrade et al., 2015; Company and Pereda-Suberbiola, 2016).

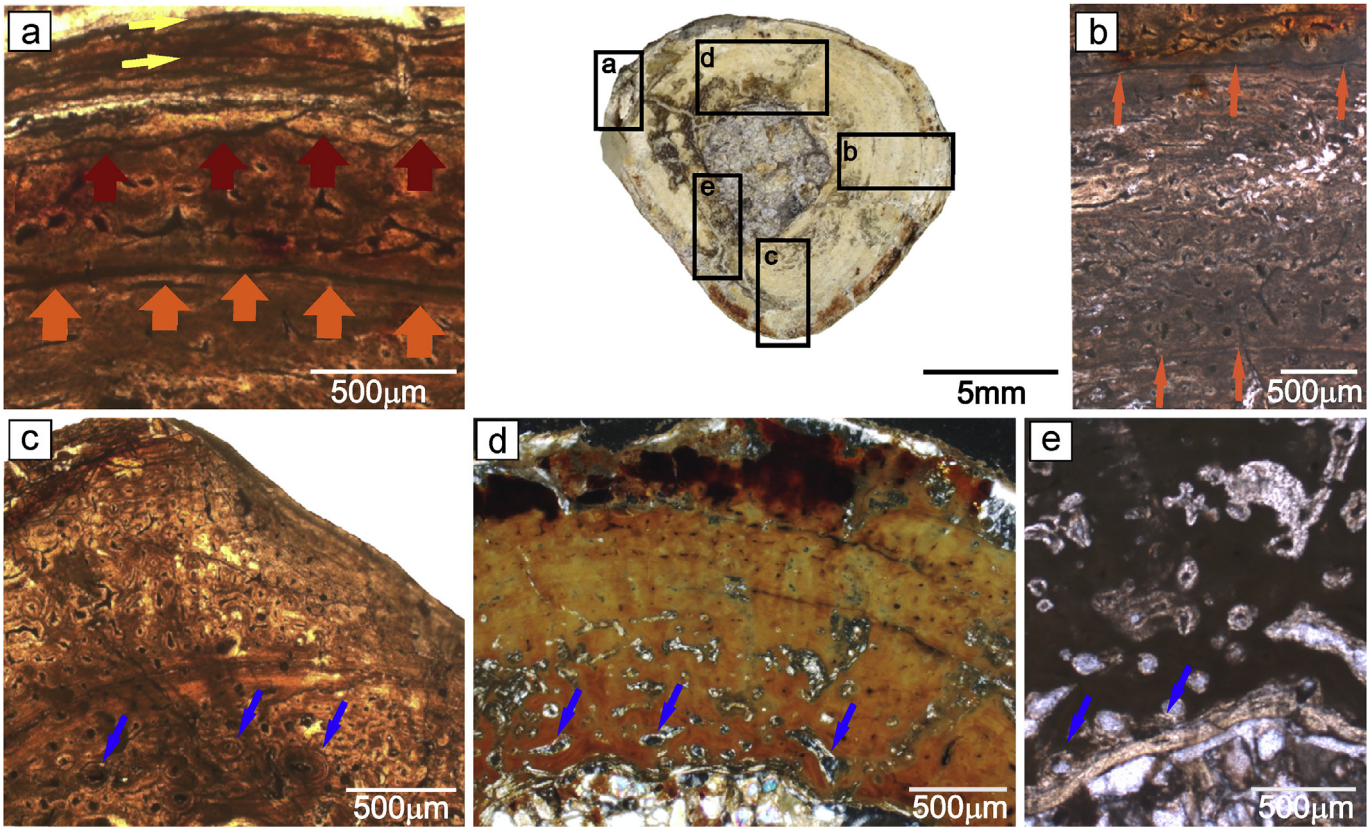


**Fig. 2.** Histological details of the femur in cross section (DP2/176). The black frames indicate the position of the areas with larger details. a) external cortex, lamellar zonal tissue, growth line indicated by orange arrows, possible growth line indicated by brown arrows and EFS indicated by yellow arrows; b) fibrolamellar primary tissue with oval to rounded primary osteons and line of arrested growth (LAG) in the medial cortex (orange arrows) c) secondary osteons (blue arrows); d) spongy tissue with reabsorption cavities; e) endosteal remodelling bone (blue arrows). (For interpretation of the references to colour in this figure legend, the reader is referred to the Web version of this article.)

The internal constitution of bones is similar in all vertebrates, with a complex anatomy in which hydroxyapatite microcrystals [$Ca_{10}(PO_4)_6(OH)_2$] are interlaced with fibres (collagen and non-collagen) that comprise between 32 and 44% of the compact bone volume (Steve-Bocciarelli, 1970; Wopenka and Pasteris, 2005; Jans, 2008; Merino and Buscalioni, 2013; Keenan, 2016). These components with several vascularization patterns are characteristic of bone microstructure. The bone microstructure and its chemical composition guarantee elasticity and resilience to the bone, which considerably contributes to the fossilization process (Jans, 2008). Due to small size and an extensive surface area (200 $m^2/g$), bone crystals have high reactivity and high dissolution rates (Weiner and Price, 1986). Therefore, bone dissolution or eventual preservation (fossilization) occurs (Trueman and Tuross, 2002). The fossildiagenesis of bones can be divided into early and late diagenesis. During the early diagenesis, the bone elements contacts geochemical and biological system, leading by necrolysis, damage to the collagen through mechanical and biotic factors, and by the influence of several chemical and structural modifications in the inorganic portion, as well as the mechanical introduction of quartz and mudstone grains (Collins et al., 1995; Nielsen-Marsh and Hedges, 2000; Trueman and Martill, 2002; Kolodny et al., 1996; Hubert et al., 1996; Trueman, 1999; Trueman et al., 2006; Keenan, 2016). In this way, during early diagenesis, the porosity and permeability allow the bones to fill with substances, and this may produce cracks in the secondary osteons, which sometimes are associated with bacterial influence (Pfretzschner, 2004; Keenan, 2016). It is worth noting that in a solution with neutral and alkaline pH, fossilization occurs easier in acid pH than alkaline because the latter dissolve the skeletal remains (Keenan and Engel, 2017).

The fossil assemblages and outcrops of Bauru Basin was mainly studied with different paleontological approaches (e.g. Bertini et al., 1993; Dias-Brito et al., 2001; Zaher et al., 2006; Pires-Domingues et al., 2007, Pinheiro et al., 2018), especially regarding the biostratinomic processes of vertebrate materials (Azevedo et al., 2013; Marinho et al., 2013; Tavares et al., 2015; Bandeira et al., 2018). However, the studies focusing in the diagenetic processes are still scarce (e.g. Batezelli et al., 2005; Azevedo et al., 2013). Therefore, the association between the depositional environment and the diagenesis are still poorly explored in Bauru Basin.

We analyzed the bone histology and taphonomy (fossil diagenesis) of isolated bones of *Montealtosuchus*. With this analysis, we could clarify aspects of the palaeoautoecology and the preservational environment of this fossil assemblage.

## 2. Material and methods

### 2.1. Geological Horizon

The Bauru Basin includes a broad area in Brazilian territory including portions of Paraná, São Paulo, Mato Grosso, Mato Grosso do Sul, Goiás, and Minas Gerais states, as well as a part of Paraguay (Batezelli, 2010). This sedimentary basin was deposited from the Cenomanian until the early Palaeocene, in semiarid conditions (Santucci and Bertini, 2001; Batezelli, 2017). This stratigraphic succession can be characterized by the Caiua, Santo Anastácio, Araçatuba, Sao José do Rio Preto, Uberaba, Adamantina, Marília and Itaqueri formations (Fig. 1).

The species *Montealtosuchus* was collected in the Adamantina

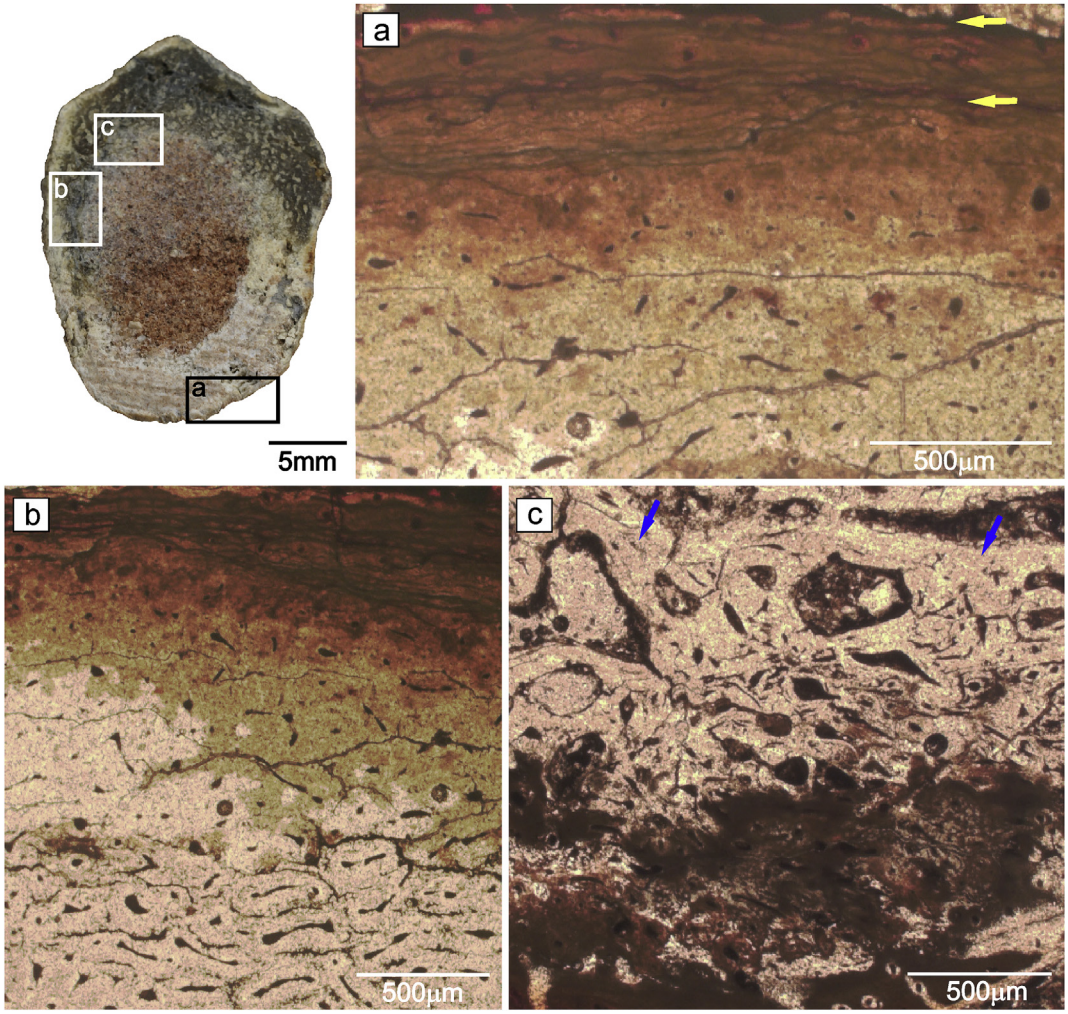


**Fig. 3.** Histological details from the vertebra in cross section (DP2/177). Black frames indicate the position of areas with larger details. a) external cortex; (EFS showing with yellow arrows); b) mid cortex with fibrolamellar primary tissue and oval to rounded primary osteons; c) spongy tissue (detail of with blue arrows). (For interpretation of the references to colour in this figure legend, the reader is referred to the Web version of this article.)

Formation, which has the deepest thickness reported so far (100 m), and it extends toward the east portion of the basin (Fernandes, 2004). This geological unit has been interpreted as a product of depositional events in lacustrine and meandering fluvian or eolian environments (e.g. with small dunes) that developed palaeosols with calcrete, ferricrete (goethite), and root tubes during non-depositional periods and had a direct influence on the variation of water table levels (Soares et al., 1980; Fernandes, 2004; Menegazzo et al., 2016; Marsola et al., 2016). The Adamantina Formation comprises fine sandstones, mostly tabular, showing several sedimentary structures (ripple cross-lamination or planar-to-trough cross stratification) with intraclasts of mudstone at the base of the troughs, interdigitated by mudstones with mudcracks, heterolithic facies, and ichnofossils (e.g. root marks and invertebrates), and with a matrix supported by intraformational conglomerates (Menegazzo et al., 2016). The sandstones consist of quartz grains moderately round and sub-rounded; feldspar and hematite grains with carbonate cement (Coelho et al., 2001; Fernandes, 2004; Batezelli, 2010).

### 2.2. Montealtosuchus (DP2/176; DP2/177; MPMA-16-0007/04)

All samples were collected by the research team from the Palaeontology Museum "Prof. Antônio Celso de Arruda Campos" (MPMA) from an outcrop located approximately 14 km from the urban area of Monte Alto (Fig. 1), on a rural road connecting to the municipality of Taiaçu (S 21° 09′53.9″W 48° 29′ 54.0″), São Paulo state.

The bones were found disarticulated and preserved in the upper sequences of the outcrop, together with at least four more fragments of cranial and several postcranial elements assigned to *Montealtosuchus*. We sampled a femur (DP2/176), a caudal vertebra (DP2/177), and the dorsal osteoderm of *Montealtosuchus* holotype (MPMA-16-0007/04) (Fig. 1C–F). The samples are housed in the Coleção de Paleontologia (DP) do Instituto de Geociências da Universidade Estadual de Campinas, UNICAMP.

### 2.3. Microscopy and element analyzes

Thin sections were produced using standard fossil histology techniques (Padian and Lamm, 2013). These thin sections were analyzed at the Laboratório de Paleohidrogeologia da UNICAMP using a petrographic microscope Carl Zeiss Scope A1 ZE/SS. The images were acquired using a ZEISS AxioCam camera and treated with the ZEISS AxioVision® 4.8.2.0. (2006) software.

The histological observations were performed with a Scanning Electron Microscopy (SEM) LEO 430i, through a digital scan of the thin sections, controlled by the software Labbok (Carl Zeiss). The chemical composition of fossilized bone was examined using Energy Dispersive Spectroscopy (EDS) Oxford. The procedure was performed at the Spectroscopy and Scanning Electron Microscopy Laboratory (MEV- IG

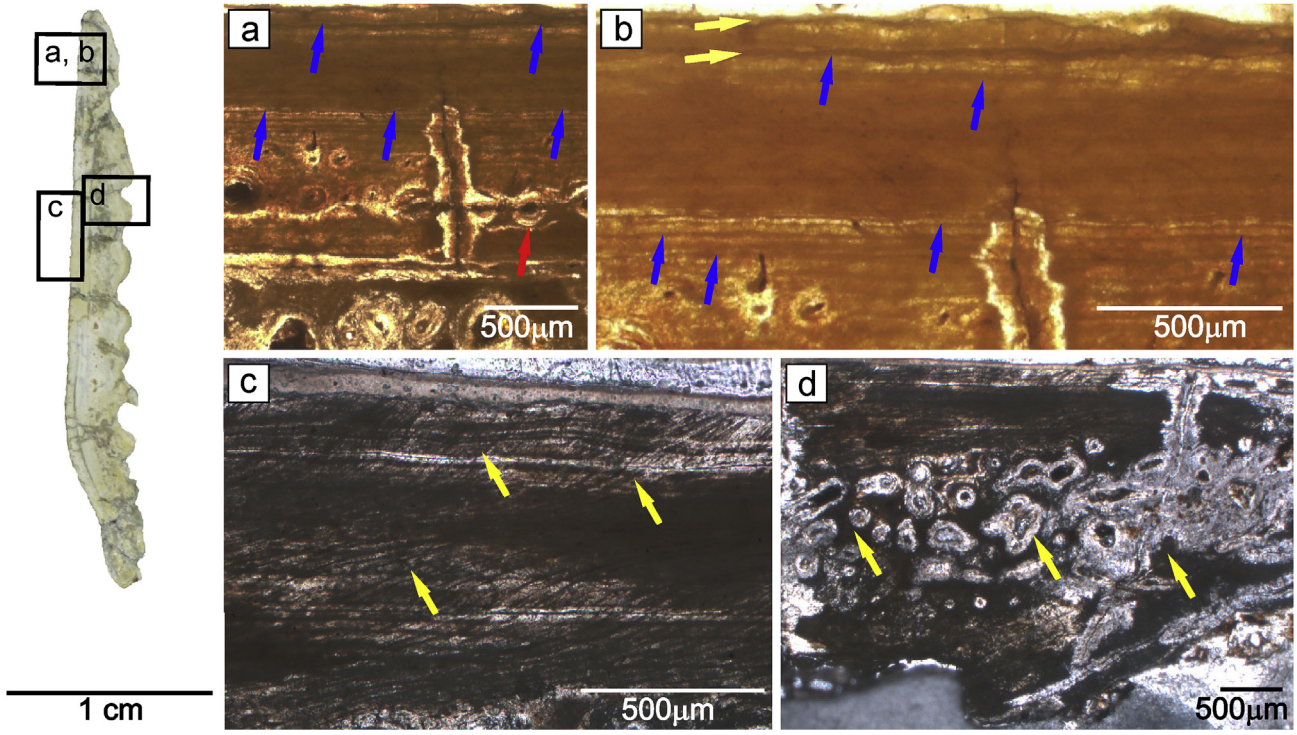


**Fig. 4.** Histological details of the osteoderm in cross section (MPMA-0007/04). Black frames indicate the position of areas with larger details. a) external cortex with lamellar tissue and LAGs (blue arrows); medial cortex with secondary osteons (red arrows); b) EFS (yellow arrows) and LAGs (blue arrows); c) cortical region with preserved sharpey fibers (yellow arrows); d) spongy tissue with reabsorption cavities (yellow arrows). (For interpretation of the references to colour in this figure legend, the reader is referred to the Web version of this article.)

-UNICAMP). The analyzes were performed using SEM equipment coupled to an EDS detector, which emphasized compositional differences to generate the images.

The µ-X-Ray Fluorescence (µ-XRF) was applied to determine the distribution of trace elements inside the femoral sample (DP2/176) to complement the SEM/EDS results. The µ-XRF analysis was performed at XRF beam line of the Brazilian Synchrotron Light Laboratory (LNLS). The instrument was operated in micro-beam mode with the Kirkpatrick-Baez mirror (KB) focusing system to attain a beam size of 12 × 25 mm diameter, at room temperature and white-beam mode of excitation. PyMca 4.6.0 software (developed by European Synchrotron Radiation Facility - ESRF) was used to treat the data and obtain the elemental maps.

## 3. Result

### 3.1. Femur – sample DP2/176

The diameter of the analyzed midshaft was 15 mm (Table, 1), which is slightly abraded. The medullary cavity was 2 mm (Table, 1), thick and filled with quartz and other mineral grains, and surrounded by remodelled endosteal bone (Fig. 2E). The spongy tissue is 2 mm (Table, 1) thick a maximum and presents reabsorption cavities (Fig. 2D), trabecular tissue, and secondary osteons (Fig. 2 C). The internal cortex was remodelled. The osteocyte density was high in the cortical region, except in the most peripheral portion, which showed no evidence of vascular channels.

Some Lines of Arrested Growth (LAGs) were observed, two in the external cortex and one in the mid cortex (Fig. 2B). The mid region of the cortex was formed by fibrolamellar primary tissue with longitudinal primary osteons (Fig. 2B).

The cortex presented a maximum thickness of 4 mm (Table, 1), of which 200 µm lied in the external cortex, composed of EFS (Fig. 2A).

### 3.2. Vertebra – sample DP2/177

The diameter of centrum was 20 mm (Table, 1). The medullar cavity presented 10 mm (Table 1) thick and was filled with rock matrix, the spongy tissue is 2 mm thick (Table, 1, Fig. 3C).

The cortical area has a maximum thickness of 3 mm (Table, 1). The medial cortex was formed by fibrolamellar primary tissue with longitudinal e reticular vascular canals (Fig. 3B). The external cortex presented few LAGs and was avascular. The density of osteocytes was high in all the cortical regions, except in the peripheral region, which showed no evidence of vascular channels and we observed the EFS in the cross section (Fig. 3A).

### 3.3. Osteoderm - SampleMPMA-16-0007/04

The dorsal osteoderm showed a transversal diameter of 4 mm (Table, 1) and 30 mm longitudinal. The spongy tissue presented few reabsorption cavities (Fig. 4D).

The spongy tissue region showed a diameter of 1,7 mm (Table, 1) while the cortex is compact and has a diameter of 0,8 mm (Table, 1). The inner cortex was formed by the primary tissue of secondary remodelling, with some secondary osteons (Fig. 4A). Along the cortical region, Sharpey's fibres were preserved (Fig. 4C). The external cortex was composed of lamellar tissue and shows an lacked vascular channels. Several LAGs were detected in the external cortex (Fig. 4A and B), and in the peripheral cortex, the EFS was observed (Fig. 4B).

The histological pattern drawn from the femur and vertebra was similar, as the internal cortex of both showed high vascularization (fibrolamellar tissue) and EFS in the external cortex. The osteoderm was not comparable with femur and vertebra due to its dermal origin (Romer, 1956).

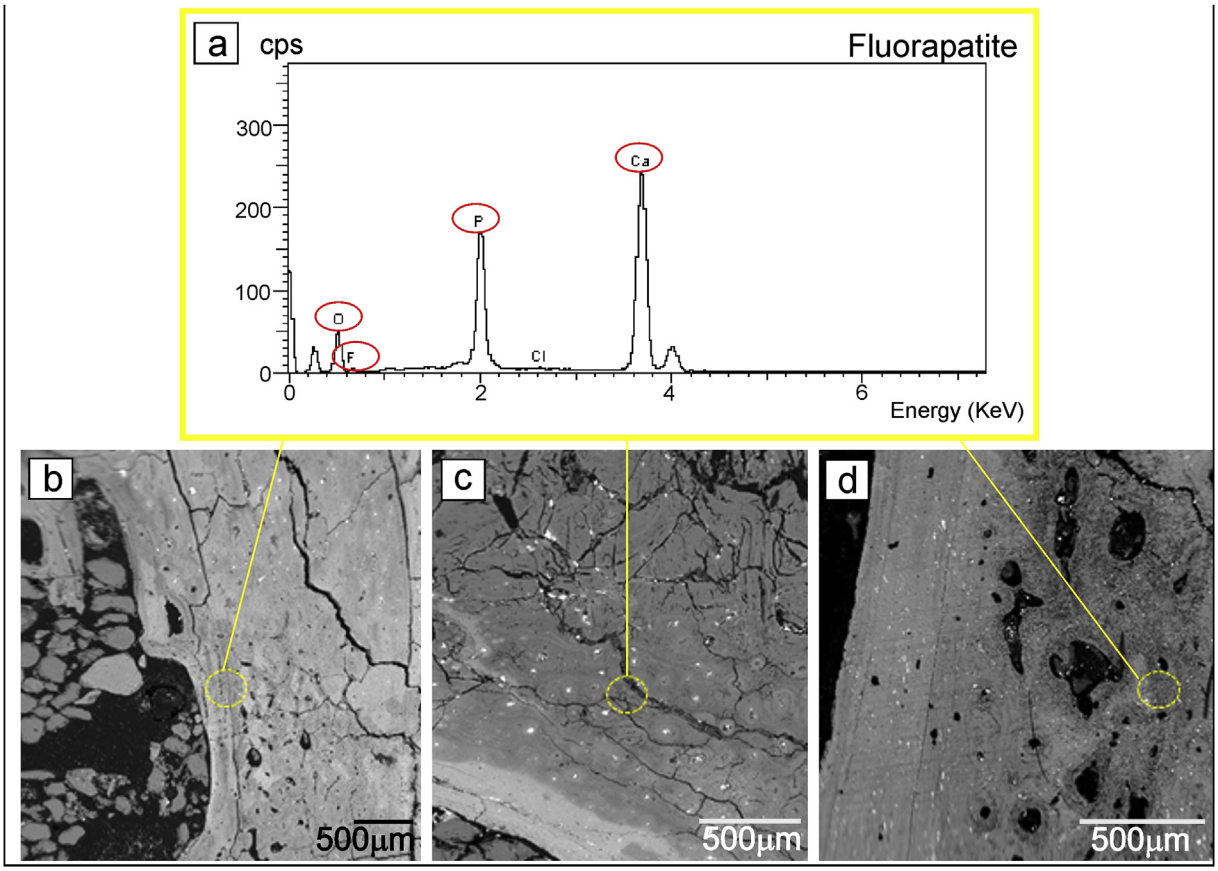


**Fig. 5.** Energy Dispersive X-Ray Spectroscopy analysis showing the general composition of the fossil (fluorapatite) and SEM images of the analyzed areas. a) EDS spectra showing the main composition of fluorapatite of the bones; the elements inside the red circles are constituents of fluorapatite; b) SEM image of femur, sample DP2/176; c) SEM image of vertebra, sample DP2/177; d) SEM image of osteoderm, sample MPMA-0007/04. Yellow circles inside the SEM images indicate the analyzed areas by EDS. (For interpretation of the references to colour in this figure legend, the reader is referred to the Web version of this article.)

### *3.4. Scanning Electron Microscopy and Energy Dispersive Spectroscopy (SEM/EDS)*

The elemental analysis showed calcium, phosphorous, oxygen, and fluorine, a composition consistent with calcium phosphate in the form of fluorapatite $Ca_5(PO_4)_3F$ that was a solid solution with hydroxyapatite $Ca_{10}(PO4)_6(OH)_2$ (Fig. 5). The osteological structures and rock matrix were filled by illite $(K,H_3O)(Al,Mg,Fe)_2(Si,Al)_4O_{10}[((OH)_2,H_2O)]$, as in the vertebra sample DP2/177 (Fig. 6). The compositional analysis in the thin sections showed dissemination of Rare Earth Elements in low concentrations (neodymium, gadolinium, and samarium), distribution of vanadium, calcium, oxygen, iron, and phosphorous, and a major concentration of cerium (Figs. 7 and 8). In the osteoderm's peripheral cortex (MPMA-16-0007/04) and in the femur (DP2/176), vanadium was detected (Figs. 7 and 8).

### *3.5. µ-X-Ray fluorescence (µ-XRF)*

The elemental map showed a distribution of elements consistent with the composition of calcium phosphate (hydroxyapatite) (Fig. 9). However, cerium was distributed all along the extension of the mapped region covering the cortex and the medullar cavity. In the peripheral cortex, iron was detected. Vanadium also showed a wide distribution throughout the fossil, but a higher concentration in the peripheral region (Fig. 9).

## 4. Discussion

### *4.1. Microstructure and ontogeny*

The taphonomic data from Tavares et al. (2015) suggest that the remains of *Montealtosuchus* could correspond until to four specimens. Our histological analyses indicate that all analyzed fossils should have belonged to one specimen, due to similar ontogenetic stage. Both cross-sections of the femur and vertebra presented fibrolamellar bone in the perimedullar region, rich in osteocyte lacunae around vascular canals which is an indicative of rapid osteogenesis (Chinsamy-Turan, 1997; Ray et al., 2012), suggesting a fast growth in this region. The tissue becomes lamellar zonal in the outer cortex, with the decrease vascularization and osteocytes, suggesting a slow growth rate, which are well known in crocodiles (Padian and Stein, 2013).

We inferred that the sampled specimens reached the adult senescence before death based on the presence of secondary osteons and EFS. This supports that the general growth rate decreased with the beginning of reproductive maturity (Sander, 2000; Ray et al., 2012). The femur and the vertebra preserved a maximum of three annual cycles due to the annual periodicity of the LAGs, zones, and annuli in many extant and extinct crocodyliforms (Chinsamy-Turan, 2005). It was not possible to infer how old were the specimens despite the fact that were observed three LAGs and several growth lines. However, due to the close space between LAGs and the bone erosion, we could not to count their exact number. Therefore we discarded the absolute number of LAGs to this skeletochronology.

The presence of EFS suggested the cessation of the asymptotic growth, assigning the skeletal maturity to the specimen (Lee and

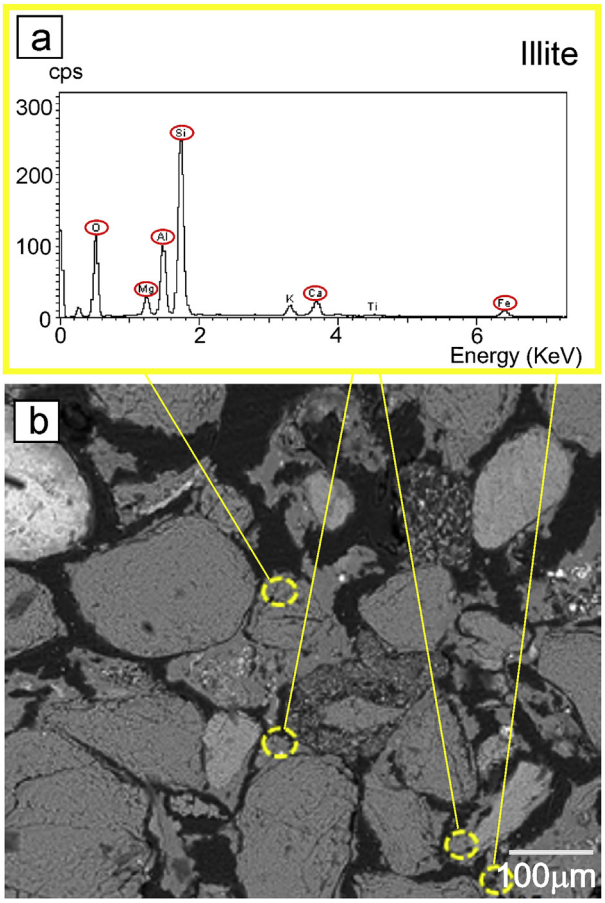


**Fig. 6.** Energy Dispersive X-Ray Spectroscopy analysis showing the illite distribution in the studied samples; SEM images of the analyzed areas. a) EDS spectra showing the points with illite. The elements that compose the illite are marked in red circles; b) SEM image of the rock matrix associated with the fossil vertebra (DP2/177). The yellow dashed circles indicate the areas where the illitic composition was determined, inside the cement. (For interpretation of the references to colour in this figure legend, the reader is referred to the Web version of this article.)

O'Connor, 2013; Andrade and Sayão, 2014). Although the indeterminate growth of reptiles can still be found in recent literature (Chinsamy-Turan, 2005; Sparkman et al., 2007), the EFS was found in several Triassic pseudosuchians (Woodward et al., 2011). The EFS reported here for Peirosauridae supports the hypothesis that determinate growth may be the rule, not the exception to archosaurs (Woodward et al., 2011).

The differential bone deposition pattern in the osteoderm does not cause any decrease or increase in the growth rate during the animal's lifespan. In the cortex, a little vascularised and lamellar zonal tissue was found, while in the central region a remodelled and thick spongy tissue was found. Growth marks in extant crocodilian osteoderms are used to determine their individual age (Tucker, 1997). For extinct taxa, they are also used as a skeletochronological tool (Hill and Lucas, 2006). In this research, at least six lines were counted (Fig. 4), which allowed a determination of 6 years as a minimal age for MPMA-16-0007/04, considering that the remodelling erased some lines. Thus, it can be inferred that this individual reached adult senescence before death.

### 4.2. Geochemical analysis and fossildiagenesis

Diagenetic processes, such as the recrystallization, dissolution–reprecipitation, or diffusion-adsorption, introduced changes in the chemical characteristics of the samples. At the beginning of the burial, during the first phase of the fossilization, quartz grains were mechanically introduced, besides feldspar, clay (illite), and lithic fragments, into the pores, fractures, and medullary cavity regions. It indicates that, during the early diagenesis, the presence of monazite or clay, verified through SEM analysis of the rocks associated with the fossils, was responsible for the presence of cerium in the burial environment. The calcium and phosphor are elements with the most concentration and uniformly distributed through the studied samples. Since the process of fossilization begins with the diagenetic recrystallization of primary crystals into apatite secondary crystals, which increases the size of the crystals (Trueman, 1999). Diagenetic recrystallization ends when all the porous spaces originally occupied by collagen were filled (Hubert et al., 1996; Trueman and Tuross, 2002). In the apatite structure, isomorphic replacements by calcium, phosphate, and hydroxide can occur, generally preserving the original morphology, and recrystallization occured close to the micropores (Pfretzschner, 2004).

Other elements found such as cerium, iron and vanadium, indicated that they were incorporated during the recrystallization, by influence of the surrounding environment (endorheic zones, confined aquifers, etc.) in which other elements with similar ionic radium sizes (e.g. Fe, Mn, Sr, Mg, Ba, Cd, and REEs) could replace the bone calcium (Herwartz et al., 2011; Keenan, 2016; Grimstead et al., 2017; Keenan and Engel, 2017).

The presence and distribution of cerium in our samples suggests that its incorporation begun during early diagenesis and continued through late diagenesis. In all the SEM/EDS analysis, the presence of apatite was verified, with the cerium present as one of the chemical components of the mineral. In the µ-XRF analysis, cerium showed a uniform distribution, being the second most abundant element in the femur after calcium. The homogeneous distribution of cerium in the compact bone reflects the state of equilibrium between the fossilizing and mineralizing bone fluids attained either by the relatively fast early diagenesis (hundreds of thousands of years) or by the prolonged (dozens of millions of years) late diagenesis distribution of REEs (Herwartz et al., 2011; Kocsis et al., 2010; Tütken et al., 2011). In the present analyses, the distribution of REEs suggest the presence of an open system that lasted after the process of early diagenesis. The growth of secondary apatite must occur in saturated waters. The chemistry of REEs is strongly influenced by the solution's pH (Byrne and Li, 1995; Johannesson and Hendry, 2000; Sonke and Salters, 2006). The saturation with apatite rarely occurs in waters with pH < 6.5. The composition of REEs in the fossil bone is controlled by the chemistry of the aqueous solution of REEs in neutral and carbonated waters (pH 8, approximately) (Trueman et al., 2006). These facts suggested that an alkaline environment was favourable for bone preservation through phosphatization, as described for Adamantina Formation (Marsola et al., 2016), with REEs not being susceptible to leaching processes.

The major and most homogeneous area of distribution of vanadium and iron is in the cortex, although they were also verified in the internal cortex. The presence of these elements in the internal cortex suggests that despite their porous nature, the bones were possibly enriched due to bacterial action, which contributed to their degradation by allowing more porosity and permeability from the external surface to the internal cortex (Millard and Hedges, 1999; Müller et al., 2011).

Vanadium is present in ground water or soil water in a wide range of pH and it tends to accumulate in the bones due to its association with calcium and phosphates, as in the case of iron (Barrio and Etcheverry, 2006; Rehder, 2013; Grimstead et al., 2017). Nevertheless, iron and vanadium could also have being incorporated by the samples during the late diagenesis for as long as ferricretes were found frequently in the Adamantina Formation layers, which attests to the variation in the water table through the Cenozoic (Coelho et al., 2001). Therefore, the alteration in the skeletal elements allowed diffusion of small quantities of vanadium and iron from the layer where they were deposited to the innermost part of the bone (Millard and Hedges, 1999). Likewise, cerium could have continued during the late diagenesis since it has a

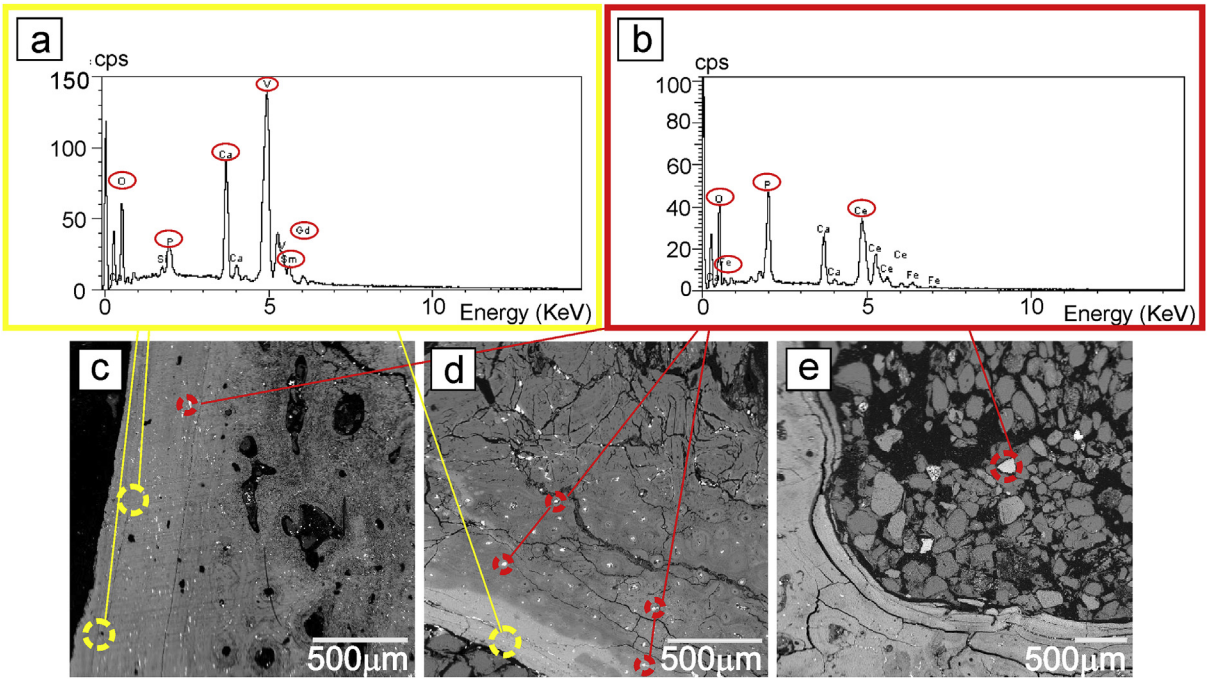


**Fig. 7.** Energy Dispersive X-Ray Spectroscopy analysis showing the REE (Samarium, Cerium and Gadolinium) and other elements (Vanadium, Calcium, Oxygen, Iron and Phosphorous) distribution in the studied samples; SEM images of the analyzed areas. a) EDS spectra indicating points with Vanadium, Calcium, Phosphorous, Oxygen, Iron, Samarium and Gadolinium composition; b) EDS spectra indicating Phosphorous, Oxygen and Cerium composition; c) Analyzed areas (dashed circles) of the external cortex from the osteoderm (MPMA-160007/04); d) analyzed areas (dashed circles) of the external cortex from the femur (DP2/176); e) analyzed areas (dashed circles) of the space filled by mineral grains in the femur marrow space (DP2/176).

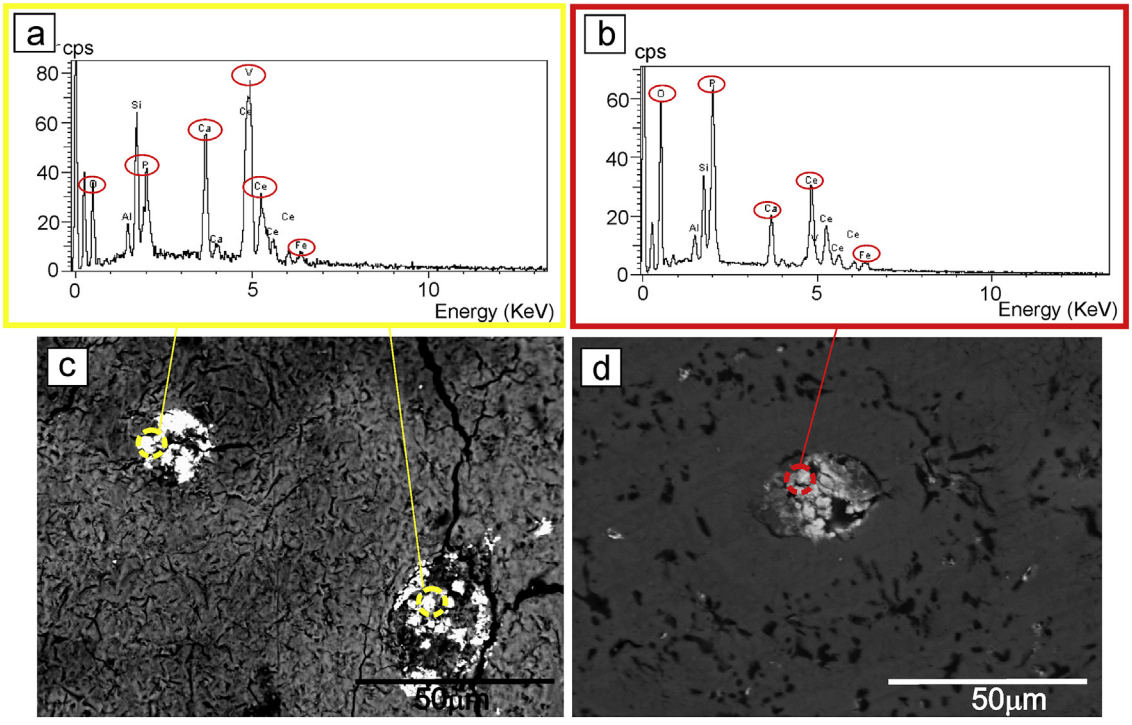


**Fig. 8.** Energy Dispersive X-Ray Spectroscopy analysis and SEM images with osteocytes filled composition. a) EDS spectra indicating Phosphorous, Calcium, Vanadium, Oxygen, Cerium and Iron; b) EDS spectra indicating Phosphorous, Calcium, Oxygen, Cerium and Iron; c) Composition of the femur vascular canals (DP2/176); d) Composition of the vertebra vascular canals (DP2/177).

homogeneous distribution. Iron and vanadium were of secondary importance for preservation because their distribution is more significant in the region of contact between the fossil and the external environment. Therefore, they probably diffused into the bone during the second phase of fossilization and diagenesis.

If the groundwater is enriched by fluoride, this will be introduced into the mineral structure, giving rise to carbonated fluorapatite [$Ca_5(PO_4CO_3)_3(F)$] or francolite [$Ca_5(PO_4)_3F$] (Hubert et al., 1996;

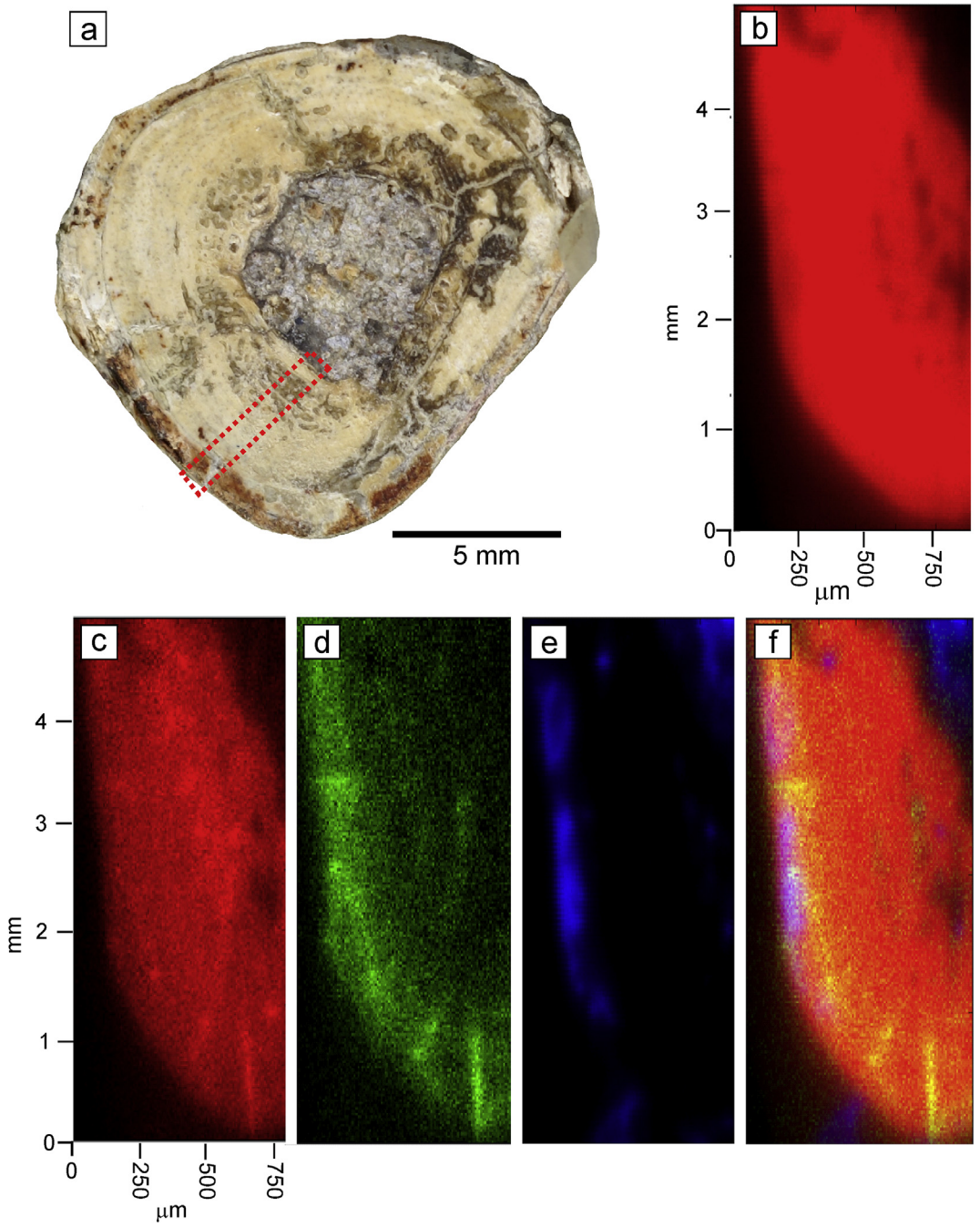


**Fig. 9.** µ- XRF elemental maps showing the distribution of the elements Calcium, Cerium, Vanadium and Iron in the femur cross section (DP2/176). a) femur cross section showing the mapped area in the sample; b) Calcium (red) distributed in all the bone cortex; c) Cerium (red), with higher intensities in the central area of the cortex; d) Vanadium (green) in a wide distribution, but higher intensity in the peripheral region; e) Iron (blue) in the peripheral cortex; f) image with the combined distribution of the mapped elements. (For interpretation of the references to colour in this figure legend, the reader is referred to the Web version of this article.)

Trueman, 1999). These minerals form a solid solution with hydroxyapatite $Ca_{10}(PO_4)_6(OH)_2$ (Fig. 6), being fluorapatite the most stable solid phase of calcium phosphate. Another chemical process that is active during diagenetic recrystallization is the diffusion–adsorption of trace elements (Millard and Hedges, 1999). Trace elements are absorbed from the outer bone surfaces and they diffuse through the porous spaces (Kolodny et al., 1996; Trueman, 1999). Nevertheless, the incorporation of REEs also could happen during late diagenesis due to the dissolution–reprecipitation processes that lead to the origin of a thermodynamically stable mineral such as fluorapatite (Herwartz et al., 2011). In the studied samples, calcium and phosphorous are the major elements, and they are evenly distributed throughout the fossils. Both have a biological origin, resulting from the original composition of bones, but they also participate in the formation of recrystallized and authigenic minerals.

## 5. Conclusions

The gradation from fast-growing tissue to low growth toward the external cortex, EFS and the secondary remodelling implies that the studied bones one individual that reached maturity ontogenetic (adult/senescent) before death.

The recrystallization that occurred during fossil diagenesis was the determining factor for bone preservation because the resulting

composition was more stable (hydroxyapatite) than the original bone composition. For a bone preservation in the fossil record, the recrystallization rate must exceed the dissolution rate. This suggests that the recrystallization was initiated during the early diagenesis in the fossilization and continued along with the incorporation of other elements such as cerium, iron, and vanadium into late diagenesis.

## Acknowledgments

The authors would like to thank the "Antônio Celso Arruda Campos" Museum, in Monte Alto, São Paulo State, Brazil, for providing the studied material; to CAPES (Brazilian Federal Agency for Support and Evaluation of Graduate Education) for the scholarship awarded and to the CNPq (National Council for Scientific and Technological Development) for the Research grant; to the CNPq (National Council for Scientific and Technological Development), FAPERJ (Carlos Chagas Filho Rio de Janeiro State Research Foundation) and FAPESP (São Paulo State Research Foundation – proposal n° 2016-20927-0) for the research funds; to the Brazilian Synchrotron Light Laboratory (LNLS) for the X-Ray Fluorescence facilities (proposal n° 20150076); to the Spectroscopy and Scanning Electron Microscopy Laboratory (MEV-IG -UNICAMP), for the SEM/EDS facilities, and to the thin section preparation laboratory from the Geosciences Institute (UNICAMP).

## Appendix A. Supplementary data

Supplementary data to this article can be found online at https://doi.org/10.1016/j.jsames.2019.102327.

## References

Andrade, M.B., Bertini, R.J., 2008. A new *Sphagesaurus* (Mesoeucrocodylia: Notosuchia) from the upper cretaceous of Monte Alto city (Bauru Basin, Brazil), and a revision of the Sphagesauridae. Hist. Biol. 20, 101–136.

Andrade, R.C.L.P., Bantim, R.A.M., Lima, F.J., Campos, L.S., Lhs, E., Sayão, J.M., 2015. New data about the presence and absence of the external fundamental system in archosaurs. Cad Cult Cien (URCA) 14 (1), 200–211.

Andrade, R.C.L.P., Sayão, J.M., 2014. Paleohistology and lifestyle inferences of a dyrosaurid (Archosauria: crocodylomorpha) from Paraíba basin (Northeastern Brazil). PLoS One 9, 102–189.

Azevedo, K.L., Vega, C.S., Fernandes, L.A., 2013. Taphonomic aspects of vertebrate fossils from Bauru Group, upper cretaceous, Brazil. Bol. Parana. Geocienc. 68–69, 43–51.

Bandeira, K.L.N., Brum, A.S., Pêgas, R.V., Cidade, G.M., Holgado, B., Cidade, A., De Souza, R.G., 2018. The Baurusuchidae vs Theropoda record in the Bauru Group (upper cretaceous, Brazil): a taphonomic perspective. J. Iber. Geol. 44, 25–54.

Barrio, D.A., Etcheverry, S.B., 2006. Vanadium and bone development: putative signaling pathways. Can. J. Physiol. Pharmacol. 84, 677–686.

Batezelli, A., Gomes, N.S., Perinotto, J.A.J., 2005. Petrografia e Evolução Diagenética dos Arenitos da Porção Norte Nordeste da Bacia Bauru (Cretáceo Superior). Rev. Bras. Geociencias 35, 311–322.

Batezelli, A., 2010. Arcabouço tectono-estratigráfico e evolução das Bacias Caiuá e Bauru no Sudeste brasileiro. Rev. Bras. Geociencias 40, 265–285.

Batezelli, A., 2017. Continental systems tracts of the Brazilian Cretaceous Bauru Basin and their relationship with the tectonic and climatic evolution of South America. Basin Res. 29, 1–25.

Bertini, R.J., Marshall, L.G., Gayet, M., Brito, P., 1993. Vertebrate faunas from the Adamantina and marilia formations (upper Bauru Group, late cretaceous, Brazil). Neues Jahrbuch fur Geologie und Paleontologie. Abhandlungen 188, 71–101.

Byrne, R.H., Li, B.Q., 1995. Comparative complexation behavior of the rare-earths. Geochem. Cosmochim. Acta 59, 4575–4589.

Carvalho, I.S., Ribeiro, L.C.B., Avilla, L.S., 2004. Uberabasuchus terrificus sp. nov. A new crocodylomorpha from the Bauru Basin (upper cretaceous), Brazil. Gondwana Res. 7 (4), 975–1002.

Carvalho, I.S., Vasconcellos, F.M., Tavares, S.A.S., 2007. Montealtosuchusarrudacamposi, a new peirosaurid crocodile (Mesoeucrocodylia) from the late cretaceous Adamantina Formation of Brazil. Zootaxa 1607, 35–46.

Chinsamy-Turan, A., 2005. The Microstructure of Dinosaur Bone. Johns Hopkins University Press, Baltimore, Maryland, pp. 195.

Chinsamy-Turan, A., 1997. Assessing the biology of the fossil vertebrates through bone histology. Palaeontol. Afr. 33, 29–35.

Coelho, M.R., Vidal-Torrado, P., Ladeira, F.S.B., 2001. Macro e micromorfologia de fericretes nodulares desenvolvidos de arenito do Grupo Bauru. Formação Admantinas. R. Bras. Ci. Solo 25, 371–385.

Collins, M.J., Riley, M.S., Child, A.M., Turner-Walker, G., 1995. A basic mathematical simulation of the chemical degradation of ancient collagen. J. Archaeol. Sci. 22, 175–183.

Company, J., Pereda-Suberbiola, X., 2016. Long bone histology of a Eusuchia crocodyliform from the Upper Cretaceous of Spain: implications for growth strategy in extinct crocodiles. Cretac. Res. 72, 1–7.

Dias-Brito, D., Musacchio, E.A., Castro, J.C., Maranhão, M.S.A.S., Suarez, J.M., Rodrigues, R., 2001. Grupo Bauru: uma unidade continental do Cretáceo no Brasil – concepções baseadas em dados micropaleontológicos, isotópicos e estratigráficos. Rèvue Paléobiologie 20, 245–304.

Fernandes, L.A., 2004. Mapa Litoestratigráfico da parte oriental da Bacia Bauru (Pr, Sp, Mg), Escala 1:1.000.000. Bol. Parana. Geocienc. 55, 53–66.

Grimstead, D.N., Clark, A.E., Rezac, A., 2017. Uranium and Vanadium concentrations as a trace elements method for identifying diagenetically altered bone in the inorganic phase. J. Archaeol. Method Theory 25, 689–704.

Herwartz, D., Tütken, T., Münker, C., Jochum, K.P., Stoll, B., Sander, P.M., 2011. Timescales and mechanisms of REE and Hf uptake in fossil bones. Geochem. Cosmochim. Acta 75, 82–105.

Hill, R.V., Lucas, S.G., 2006. New data on the anatomy and relationships of the Paleocenecrocodylian Akanthosuchuslangstoni. Acta Palaeontol. Pol. 51, 455–464.

Hubert, J.F., Panish, P.T., Chure, D.J., Prostak, K.S., 1996. Chemistry, microstructure, petrology, and diagenetic model of Jurassic dinosaur bones, Dinosaur National Monument, Utah. J. Sediment. Res. 66, 531–547.

Iori, F.V., Carvalho, I.S., 2009. Morrinhosuchusluziae, um novo Crocodylomorpha Notosuchia da Bacia Bauru, Brasil. Rev. Bras. Geociencias 39, 717–725.

Iori, F.V., Carvalho, I.S., 2011. Caipirasuchuspaulistanus, a new sphagesaurid(crocodylomorpha, Mesoeucrocodylia) from the Adamantina Formation (upper cretaceous, Turonian-Santonian), Bauru Basin, Brazil. J. Vertebr. Paleontol. 31, 1255–1264.

Iori, V.F., Garcia, K.L., 2012. Barreirosuchusfranciscoi, um novo CrocodylomorphaTrematochampsidae da Bacia Bauru, Brasil. Rev. Bras. Geociencias 42, 397–410.

Jans, M.M., 2008. Microbial bioerosionofbone–a review. In: Wisshak, M., Tapanila, L. (Eds.), Current Developments in Bioerosion. Springer, Berlin, Heidelberg, Current Developments in Bioerosion. Erlangen Earth Conference Series, pp. 397–413.

Johannesson, K.H., Hendry, M.J., 2000. Rare earth element geochemistry of groundwaters from a thick clay and till-rich aquitard sequence, Saskatchewan, Canada. Geochem. Cosmochim. Acta 64, 1493–1509.

Keenan, W.S., 2016. From bone to fossil: a review of the diagenesis of bioapatite. Am. Mineral. 101, 1943–1951.

Keenan, W.S., Engel, A.S., 2017. Early diagenesis and recrystallization of boné. Geochem. Cosmochim. Acta 196, 209–223.

Klein, N., Scheyer, T., Tütken, T., 2009. Skeletochronology and isotopic analysis of a captive individual of Alligator mississippiensis Daudin, 1802. Fossil Rec. 12 (2), 121–131.

Kocsis, L., Trueman, C.N., Palmer, M.R., 2010. Protracted diagenetic alteration of REE contents in fossil bioapatites: direct evidence from Lu-Hf isotope systematics. Geochem. Cosmochim. Acta 74, 6077–6092.

Kolodny, Y., Luz, B., Sander, M., Clemens, W.A., 1996. Dinosaur bones: fossils or pseudomorphs? The pitfalls of physiology reconstruction from apatitic fossils. Palaeogeogr. Palaeoclimatol. Palaeoecol. 126, 161–171.

Lee, A.H., O'Connor, P.M., 2013. Bone histology confirms determinate growth and small body size in the noasaurid theropod Masiakasaurus knopfleri. J. Vertebr. Paleontol. 33 (4), 865–876.

Marinho, T.S., 2006. Osteodermos de crocodilomorfos e dinossauros da Bacia Bauru (Cretáceo Superior) (Ph.D. dissertation). Instituto de Geociências, UFRJ 52pp.

Marinho, T.S., Iori, F.V., Carvalho, I.S., Vasconcellos, F.M., 2013. Gondwanasuchusscabrosus gen. et sp. nov., a new terrestrial predatory crocodyliform (Mesoeucrocodylia: Baurusuchidae) from the Late Cretaceous Bauru Basin of Brazil. Cretac. Res. 44, 104–111.

Marsola, J.C.A., Batezelli, A., Felipe, C., Montefeltro, F.C., Gellet-Tinner, G., Langer, M.C., 2016. Palaeoenvironmental characterization of a crocodilian nesting site from the Late Cretaceous of Brazil and the evolution of crocodyliform nesting strategies. Palaeogeogr. Palaeoclimatol. Palaeoecol. 457, 221–232.

Martine, A.M., 2013. Reconstituições paleoartísticas da Bacia Bauru, Paraná e Araripe (Ph.D. dissertation). Instituto de Geociências, Universidade de Campinas, pp. 120.

Martinelli, A.G., Marinho, T.S., Iori, F.V., Ribeiro, L.C.B., 2018. The first *Caipirasuchus* (Mesoeucrocodylia, Notosuchia) from the late cretaceous of Minas Gerais, Brazil: new insights on sphagesaurid anatomy and taxonomy. PeerJ 6, e5594.

Menegazzo, M.C., Catuneanu, O., Chang, H.K., 2016. The South American retroarc foreland system: the development of the Bauru Basin in the back-bulge province. Mar. Pet. Geol. 73, 131–156.

Merino, L., Buscalioni, A.D., 2013. Mineralogía y cambios composicionales en fragmentos óseos atribuidos a un dinosaurio ornitópodo del yacimiento barremiense de Buenache de la Sierra (Formación Calizas de La Huérguina, Cuenca, España). Estud. Geol. 69, 193–207.

Millard, A.R., Hedges, R.E.M., 1999. A diffusion-adsorption model of uranium uptake by archaeological bone. Geochem. Cosmochim. Acta 60, 2139–2152.

Müller, K., Chadefaux, C., Thomas, N., Reiche, I., 2011. Microbial attack of archaeological bones versus high concentrations of heavy metals in the burial environment. A case study of animal bones from a mediaeval copper workshop in Paris. Palaeogeogr. Palaeoclimatol. Palaeoecol. 310, 39–51.

Nascimento, P.M., Zaher, H., 2010. A new species of *Baurusuchus* (Crocodyliformes, Mesoeucrocodylia) from the Upper Cretaceous of Brazil, with the first complete postcranial skeleton described for the family Baurusuchidae. Papéis avulsos de Zoologia 50 (21), 323–361.

Nielsen-Marsh, C.N., Hedges, R.E.M., 2000. Patterns of diagenesis in bone I: the effects of site environments. J. Archaeol. Sci. 27, 1139–1150.

Padian, K., Stein, K., 2013. Evolution of growth rates and their implications. In: Padian, K., Lamm, E.T. (Eds.), Bone Histology of Fossil Tetrapods: Advancing Methods,

Analysis, and Interpretation. University of California Press, Berkeley, pp. 253–264.
Padian, K., Lamm, E.T., 2013. Bone Histology of Fossil Tetrapods: Advancing Methods, Analysis, and Interpretation. University of California Press, Berkeley, pp. 55–160.
Pfretzschner, H.U., 2004. Fossilization of Haversian bone in aquatic environments. Comptes Rendus Palevol 3, 605–616.
Pinheiro, A.E.P., Pereira, P.V.L.G., Da, C., De Souza, R.G., Brum, A.S., Lopes, R.T., Machado, A.S., Bergqvist, L.P., Simbras, F.M., 2018. Reassessment of the enigmatic crocodyliform "*Goniopholis*" *paulistanus* Roxo, 1936: historical approach, systematic, and description by new materials. PLoS One 13, e0199984.
Pires-Domingues, R.A., Nascimento, P.M., Simões, M.G., Ricomini, C., Zaher, H., 2007. Implicações dos dados Geológicos, Fossilíferos e Tafonômicos nas Reconstruções da Fauna de Vertebrados da Bacia Bauru: Uma Abordagem Integrada. In: Paleontologia: Cenário da Vida, vol. 2. Interciências, pp. 273–284.
Pol, D., Nascimento, P.M., Carvalho, A.B., Riccomini, C., Pires-Domingues, R.A., Zaher, H., 2014. A new notosuchian from the Late Cretaceous of Brazil and the phylogeny of advanced notosuchians. PLoS One 9 (4), e93105.
Ray, S., Botha-Brink, J., Chinsamy-Turan, A., 2012. Dicynodont growth dynamics and lifestyle adaptations. In: Chinsamy-Turan, A. (Ed.), Forerunners of Mammals. Indiana Academic Press, Bloomington, pp. 121–148.
Rehder, D., 2013. The future of/for vanadium. Dalton Trans. 42, 11749–11761.
Romer, A.S., 1956. Osteology of the Reptiles. Krieger Publishing Company, Florida.
Sander, P.M., 2000. Long bone histology of the Tendaguru sauropods: implications for growth and biology. Paleobiology 26, 46–488.
Santucci, R.M., Bertini, R.J., 2001. Distribuição Paleogeográfica e Biocronológica dos Titanossauros (Saurishia, Sauropoda) do Grupo Bauru, Cretáceo Superior do Sudeste Brasileiro. Rev. Bras. Geociencias 31, 307–315.
Sayão, J.M., Bantim, R.A.M., Andrade, R.C.L.P., Lima, F.J., Saraiva, A.A.F., Figueiredo, R.R.G., 2016. Paleohistology of Susisuchus anatoceps (Crocodylomorpha, Neosuchia): comments on growth strategies and lifestyle. PLoS One 11 (5), e0155297.
Sparkman, A.M., Arnold, S.J., Bronikowski, A.M., 2007. An empirical test of evolutionary theories for reproductive senescence and reproductive effort in the garter snake Thamnophis elegans. Proc. R. Soc. Lond. B Biol. Sci. 274 (1612), 943–950.
Soares, P.C., Landim, P.M.B., Fulfaro, V.J., Neto, A.S., 1980. Ensaio de caracterização estratigráfica do Cretáceo no estado de São Paulo: Grupo Bauru. Braz. J. Genet. 10, 177–185.
Sonke, J.E., Salters, V.J.M., 2006. Lanthanide-humic substances complexation. I. Experimental evidence for a lanthanide contraction effect. Geochem. Cosmochim. Acta 70, 1495–1506.
Steve-Bocciarelli, D., 1970. Morphology of crystallites in bone. Calcif. Tissue Res. 5, 261.
Tavares, S.A.S., Branco, F.R., Carvalho, I.S., 2015. Osteoderms of Montealtosuchus arrudacaposi (Crocodyliformes, Peirosauridae) from the Turonian-Santonian (upper cretaceous) of Bauru Basin, Brazil. Creat. Res. 56, 651–661.
Trueman, C.N., 1999. Rare earth element geochemistry and taphonomy of terrestrial vertebrate assemblages. Palaios 14, 555–568.
Trueman, C.N., Behrensmeyer, A.K., Potts, R., Tuross, N., 2006. High-resolution records of location and stratigraphic provenance from the rare earth element composition of fossil bones. Geochem. Cosmochim. Acta 70, 4343–4355.
Trueman, C.N., Martill, D.M., 2002. The long term preservation of bone: the role of bioerosion. Archaeometry 44, 371–382.
Trueman, C.N., Tuross, N., 2002. Trace elements in recent and fossil bone apatite. Rev. Mineral. Geochem. 48, 489–521.
Tucker, A.D., 1997. Validation of skeletochronology to determine age of freshwater crocodiles (Crocodylus johnstoni). Mar. Freshw. Res. 48, 343–351.
Tütken, T., Vennemann, T.W., Pfretzschner, H.U., 2011. Nd and Sr isotope compositions in modern and fossil bones–Proxies for vertebrate provenance and taphonomy. Geochem. Cosmochim. Acta 75, 5951–5970.
Weiner, S., Price, P.A., 1986. Disaggregation of bones into crystals. Calcif. Tissue Int. 39, 365–375.
Woodward, H.N., Horner, J.R., Farlow, J.O., 2011. Osteohistological evidence for determinate growth in the American Alligator. J. Herpetol. 45, 339–342.
Wopenka, B., Pasteris, J.D., 2005. A mineralogical perspective on the apatite in bone. Mater. Sci. Eng. C25, 131–143.
Zaher, H., Pol, D., Carvalho, A.B., Riccomine, C., Campos, D., Nava, W., 2006. Redescription of the cranial morphology of *Mariliasuchusamarali* and its phylogenetic affinities (Crocodyliformes, Notosuchia). Am. Mus. Novit. 3512, 1–40.